Biochemical and Biophysical Research Communications 377 (2008) 62–67

Contents lists available at ScienceDirect

Biochemical and Biophysical Research Communications

journal homepage: www.elsevier.com/locate/ybbrc

DNA-directed assembly of artificial multienzyme complexes

Joachim Müller, Christof M. Niemeyer *

Technische Universität Dortmund, Fakultät Chemie, Biologisch-Chemische Mikrostrukturtechnik, Otto-Hahn Str. 6, D-44227 Dortmund, Germany

ARTICLE INFO

Article history:
Received 8 September 2008
Available online 25 September 2008

Keywords:
DNA conjugate
Enzyme
Glucose oxidase
Horseradish peroxidase
Substrate channeling
Multienzyme complex

ABSTRACT

This study aims to establish model systems for the exploration of proximity effects, occurring in natural multienzyme complexes. DNA-directed assembly of covalent conjugates of DNA oligonucleotides and Glucose Oxidase (GOX) or Horseradish peroxidase (HRP) was used to generate supramolecular complexes, in which the two enzymes were arranged with defined spatial orientation. Electrophoretic studies indicated that the assembly efficiency significantly depends on positional and sterical factors of the two DNA–enzyme conjugates. Kinetic rate measurements of the coupled reaction of glucose oxidation and Amplex Red peroxidation were carried out with microplate-immobilized DNA–GOX–HRP complexes, and the influence of Catalase on this reaction was determined. The kinetic measurements revealed a significant increase in the reactivity of the complexes, in which GOX and HRP were immobilized in direct proximity on a complementary DNA carrier.

© 2008 Elsevier Inc. All rights reserved.

Multienzyme complexes are large polypeptides with defined tertiary and quaternary structure, which comprise multiple catalytic centers [1]. These complexes are abundant in nature, and prominent examples include fatty acid synthase [2,3], tryptophan synthase [4,5], or non-ribosomal peptide and polyketide synthases [6,7]. Multienzyme complexes display distinct advantages over isolated enzymes during a sequential multistep transformation of a substrate. In particular, the close proximity of active sites leads to mechanistic advantages because reactions limited by the rate of diffusional transport are accelerated and the "substrate-channeling" of intermediate products also avoids side reactions [8]. Thus, creation and engineering of artificial multienzyme complexes for potential applications in biocatalysis represents a challenging goal. A feasible approach to develop artificial multienzyme complexes is based on protein engineering, often combined with methods of directed evolution [9–11]. Because this approach essentially requires large efforts in protein chemistry, we have previously suggested that semisynthetic conjugates of enzymes tagged with short DNA oligonucleotides might be used to rapidly assemble multienzyme complexes by virtue of complementary Watson–Crick base-pairing [12]. Such a DNA-directed assembly of DNA–enzyme conjugates would offer a high degree of modularity and spatial control, which is otherwise not accessible by conventional chemical cross-linking. Although many semisynthetic DNA–enzyme conjugates have meanwhile been developed [13], examples of DNA-assembled multienzymes are still scarce. One marked example concerns the DNA-directed assembly of a bienzyme complex comprised of luciferase and oxidoreductase, which catalyzed the consecutive reactions of flavinmononucleotide reduction and aldehyde oxidation [14]. Indeed, overall enzymatic activity of this complex depended on the absolute and relative spatial orientation of the two enzymes.

Because such studies are useful to explore proximity effects in biochemical pathways and they might also lead to the development of artificial multienzymes as novel biocatalysts, we here report on the DNA-directed assembly and kinetic analysis of a bienzyme system comprised of Glucose Oxidase (GOX) and Horseradish peroxidase (HRP). The GOX–HRP system combines the oxidation of glucose to gluconolactone and H_2O_2 by GOX with the subsequent transformation of H_2O_2 and the fluorogenic dye Amplex Red to form highly fluorescent resorufin by HRP (Fig. 1A). The GOX–HRP system has often been used as a reporter system in biosensing [15,16] or as a model to develop microfluidic [17] or logical [18] devices. However, to the best of our knowledge, no detailed investigation of spatial coupling of these two enzymes has been reported so far. We here employ the DNA-directed assembly of covalent DNA conjugates GOX and HRP to generate several supramolecular complexes (**1**–**4**, in Fig. 1B) on the surface of microtiterplates. The complexes were analyzed by measuring the kinetic rates for the two-step reaction shown in Fig. 1A. Moreover, the influence of Catalase on this reaction was determined. Our results show clear evidence of improved reactivity of complexes, in which GOX and HRP are immobilized in direct proximity on a complementary DNA carrier strand.

Materials and methods

Chemicals. Horseradish peroxidase (HRP; purity number of 3) and Glucose Oxidase (GOX, from *Asparagillus niger*) were purchased

* Corresponding author. Fax: + 49 231 755 7082.
E-mail address: christof.niemeyer@tu-dortmund.de (C.M. Niemeyer).

0006-291X/$ - see front matter © 2008 Elsevier Inc. All rights reserved.
doi:10.1016/j.bbrc.2008.09.078

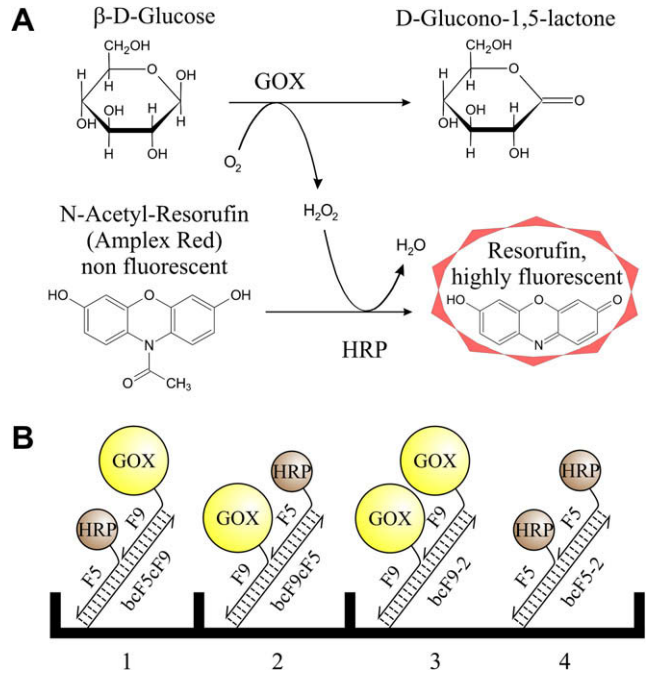

Fig. 1. Design of complexes. The mechanism of the coupled enzymes (A) includes the initial reaction of Glucose Oxidase (GOX) to oxidize Glucose to Glucono-1-lacton while producing H_2O_2. In the second step, Horseradish Peroxidase (HRP) reduces the H_2O_2 to water and the substrate *N*-Acetyl-resorufin (Ampex Red) is oxidized to form the highly fluorescent product Resorufin. Four different complexes were assembled by DNA-directed immobilization on microplate surfaces (B). Complex **1** and **2** contain the two enzymes in two different arrangements, while in control experiments, similar amounts of the enzymes were assembled in a pairwise homodimeric fashion (complex **3** and **4**), to account for differences in hybridization efficiency which result from positional and sterical influences (see text for details). Note that the arrows indicate the 3′–5′ direction of DNA and that enzymes are approximately drawn to scale. The oligonucleotide sequences are listed in Table 1.

from Sigma–Aldrich. Sulfo-succinimidyl-4-(*N*-maleimido-methyl)-cyclohexan-1-carboxylate (sSMCC) was obtained from Pierce, Amplex Red was purchased from Invitrogen. Oligonucleotides SHF5, SH-T6F5, SHF9, SH-T6F9, SH-3'-F9, bcF5cF9, bcF9cF5, bcF9-2 and bcF5-2 were from Sigma–Aldrich, sequences are listed in Table 1.

Synthesis of DNA–Enzyme-Conjugates. DNA–HRP-conjugates were synthesized from HRP and thiolated DNA-oligonucleotide SH-F5, as described earlier [19]. The same protocol was used for the synthesis of GOX-conjugates, using GOX and thiolated oligonucleotide SH-F9 (for sequences, see Table 1). In brief, the enzyme was activated with sSMCC, purifed by size-exclusion chromatography and mixed with a solution of the thiolated oligonucleotide.

Table 1
Used DNA Sequences

Abbreviation	Sequence
bcF5cF9	5′Biotin-CTT ATC GCT TTA TGA CCG GAC CCT TCA CGA TTG CCA CTT TCC AC
bcF9cF5	5′Biotin-CTT CAC GAT TGC CAC TTT CCA CCT TAT CGC TTT ATG ACC GGA CC
bcF9-2	5′Biotin-CTT CAC GAT TGC CAC TTT CCA CCT TCA CGA TTG CCA CTT TCC AC
bcF5-2	5′Biotin-CTT ATC GCT TTA TGA CCG GAC CCT TAT CGC TTT ATG ACC GGA CC
F5	5′-GGT CCG GTC ATA AAG CGA TAA G
F9	5′-GTG GAA AGT GGC AAT CGT GAA G
T6-F5	5′-TTT TTT GGT CCG GTC ATA AAG CGA TAA G
T6-F9	5′-TTT TTT GTG GAA AGT GGC AAT CGT GAA G

Subsequent to incubation for 3 h, the mixture was concentrated by ultrafiltration. Conjugates were purified by anion-exchange chromatography [19] and quantified spectrophotometrically (Cary 100 Bio), using $\varepsilon_{405} = 102\ mM^{-1}\ cm^{-1}$ for HRP [20] and $\varepsilon_{450} = 28.2\ mM^{-1}\ cm^{-1}$ [21] for GOX conjugates.

Gelelectrophoretic binding studies. Samples for gelelectrophoretic analyses (Fig. 2, see also Supplementary material S1) were prepared by mixing respective amounts of enzyme conjugates and complementary oligonucleotide carrier strands in a total volume of 10 µl in TBS buffer (150 mM NaCl, 20 mM Tris, pH 7.3). The samples were incubated for 30 min at room temperature. After adding 2 µl 6× tracking dye (Massruler Loading Dye #R0631, Fermentas), the samples were loaded on a precasted 4–20% Tris–HCl gradient polyacrylamidgel (Biorad). 10 µl 50 bp ladder (O'Range #0613, Fermentas) was used as marker. Electrophoresis was performed at 4 °C under constant 120 V for 2.5 h. The bands were visualized using the Sybr Gold staining kit (Molecular Probes).

Kinetic measurements. Supramolecular DNA–bienzyme complexes **1**–**4** (Fig. 1B) were assembled in wells of microplates, containing the complementary carrier strands. The microplates were prepared by initial coating with Streptavidin (STV) and subsequent binding of biotinylated capture oligomers bcF9cF5, bcF5cF9, or as control, an equimolar mixture of cF9-2 and cF5-2, using the previously described protocol [22]. Subsequent to immobilization, 150 fmol of the DNA–enzyme conjugates were allowed to bind for 90 min. The plate was washed with TETBS (150 mM NaCl, 20 mM Tris, 5 mM EDTA, 0.05% Tween 20, pH 7.3), and Kpi300 (50 mM Potassiumphosphat, 300 mM NaCl, pH 7.4) buffer. To start the reaction, 100 µl of substrate solution, containing 1 mM glucose, 20 µM Amplex Red in KPi300 and optional 1 µM Catalase were added to each well. The fluorescence emission was monitored continuously at 590 nm (λ_{ex} 530 nm) in a Microplate Reader (Synergy II, Biotek), and initial rates were determined using the associated Software Gen5 (Biotek). Typically, data were determined by at least four independent measurements.

Results and discussion

Synthesis and assembly of DNA–enzyme conjugates

To assemble the supramolecular DNA–enzyme complexes **1**–**4**, depicted in Fig. 1B, covalent conjugates of GOX and HRP and 5′-thiolated oligonucleotides F9 and F5, respectively, were synthesized as previously described [19]. Oligonucleotide sequences of F9, F5, and of the complementary carrier strands bcF5, bcF9, bcF5cF9, bcF9cF5, bcF9-2, and bcF5-2, were chosen due to their highly specific and uniform hybridization efficiency [23,24]. In addition to the conjugates GOX-F9 and HRP-F5, additional conjugates of GOX and HRP were synthesized from oligonucleotides comprising a T_6-spacer in between the alkylthiol group and the 5′-end of the coding sequence. These conjugates were termed as GOX-T6-F9 and HRP-T6-F5. To analyze influences of steric constraints, one additional conjugate of GOX was synthesized, in which the enzyme was linked to the 3′-end of the oligomer F9 (GOX-3′-F9).

To initially investigate the DNA-directed assembly of GOX- and HRP-conjugates, experiments in homogeneous solution were performed and analyzed by native polyacrylamide gelelectrophoresis (Fig. 2). To study effects of the spatial arrangement on the efficiency of DNA-directed assembly, GOX-F9 and GOX-3′-F9 conjugates were used, in which GOX was linked to either the 5′- or the 3′-end, respectively, of the oligonucleotide F9. As shown in Fig. 2, all three enzyme conjugates revealed a single band (lanes 1, 9, and 14), which indicated their integrity and purity. Addition of carrier oligomer led to slight changes in electrophoretic mobility and increased band intensities, due to higher DNA content of these

7 pmol each	1	2	3	4	5	6	7	8	9	10	11	12	13	14	15
GOX-F9	X	X		X	X	X									
GOX-3'F9			Marker							X	X	X	Marker	X	X
HRP-F5				X	X	X		X	X	X	X	X			
DNA (bcF5cF9)		X		0.5eq	1eq	2eq	X	X		0.5eq	1eq	2eq			X

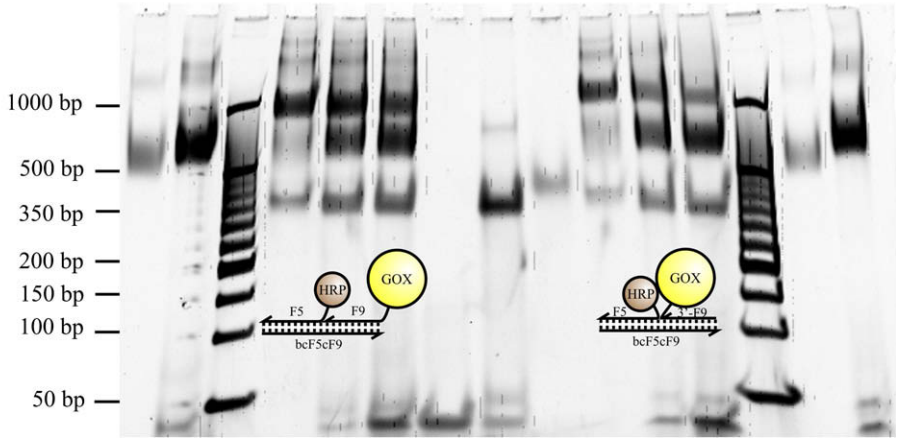

Fig. 2. In solution analysis of the DNA-directed assembly of GOX- and HRP-conjugates by native polyacrylamide gelelectrophoresis using a gradient gel (4–20%) and Sybr Gold staining. Two different GOX-F9 conjugates were used, in which GOX was linked to either the 5′- (GOX-F9) or the 3′-end (GOX-3′-F9) of F9 oligomer, to analyze influences of steric constraints. Lane 1: GOX-F9; lane 2: GOX-F9 and bcF5cF9; lane 3 and 13: marker (50 bp ladder, Fermentas); lanes 4–6: GOX-F9 and HRP-F5 with 0.5, 1, or 2 equivalents of carrier bcF5cF9, respectively; lane 7: carrier bcF5cF9; lane 8: HRP-F5 and carrier bcF5cF9; lane 9: HRP-F5; lanes 10–12: GOX-3′-F9 and HRP-F5 with 0.5, 1, or 2 equivalents of carrier bcF5cF9, respectively; lane 14: GOX-3′-F9; lane 15: GOX-3′-F9 and carrier bcF5cF9. Note that significant amount of unbound conjugate is present in the equimolar mixture (lanes 5 and 11) and the hybridization efficiency is greater in head-to-tail (lanes 4–6) than in the head-to-head configuration (lanes 10–12).

conjugates (lanes 2, 8, and 15). This result suggested undisturbed hybridization capability of the DNA–enzyme conjugates. In the simultaneous assembly of two conjugates, however, significant amounts of unbound conjugates were observable (lanes 4–6 and 10–12), even in the equimolar mixture of the three components (lanes 5 and 11). Moreover, formation efficiency of the ternary complexes was greater in head-to-tail (lanes 4–6) than in the head-to-head configuration (lanes 10–12). These results indicated that the formation of supramolecular complexes is incomplete, likely due to the presence of dissociation/association equilibria [25], which depend on spatial and sterical properties of the assembled compounds.

Similar experiments were also carried out using conjugates GOX-T6-F9 and HRP-T6-F5, which contain a T_6-spacer in between the enzyme and the DNA (see Supplementary material Fig. S1). While conjugate purity, integrity and hybridization to the carrier only was similar to the analogous conjugates lacking the spacer, the effect of the T_6-spacer was evident from the fact that lower amounts of unbound conjugates were present in the equimolar mixture (Fig. S1, lane 6), as compared to the conjugates without the spacer (Fig. 2, lanes 5, and 11). Again, this observation supported the conclusion that steric demand of the compound tethered to the oligomer markedly affects the hybridization process.

Due to the proposed equilibria, and thus the presence of unbound conjugates, we reasoned that putative channeling effects might be difficult to observe by in-solution measurements. Indeed, kinetic analyses of supramolecular GOX–HRP–DNA complexes in solution revealed only negligible effects (data not shown). To account for this problem, we decided to assemble complexes **1**–**4** on surfaces of a microplate (Fig. 1B), thus allowing to wash away unbound enzyme conjugates. To initially study hybridization efficiency of the concatenated carrier strands bcF5cF9 and bcF9cF5, embedded in complexes **1** and **2**, we employed two GOX–DNA conjugates as reporters, in which the enzyme was either linked to oligomer F5 or F9 (GOX-F5 and GOX-F9, respectively, in Fig. 3). Subsequent to DNA-directed immobilization of GOX-F5 and/or GOX-F9 on the two carriers, GOX activity was determined, using a solution containing fixed concentrations of Glucose, Amplex Red, and native HRP. As shown in Fig. 3, enzymatic activity values, and thus hybridization efficiency of GOX, were dependent on the distance to the surface. Hybridization to carrier stretches close to the surface was about 30% less efficient than to stretches further away from the surface. Likely, this occurred due to greater sterical hindrance of the adjacent surface and the dangling end of the carrier. It was also evident that, when both enzymes were allowed to hybridize with a single carrier, hybridization efficiency was only about 80% of what one would expect by summing up the signals obtained from the single conjugate experiments (100%). The latter result was likely due to steric repulsion of the two bulky enzyme moieties. To account for the incomplete hybridization due to positional and steric effects, the controls for the kinetic measurements were designed such, that two enzymes were assembled in a homodimeric fashion (Fig. 1B). Thus, an equimolar mixture of two concatenated capture oligomers (bcF9-2 and bcF5-2) was used in the controls. The sequences contained a twofold repetition of either the cF9- or cF5-sequence motif for the assembly of complex **3** and **4**, respectively, in Fig. 1B.

Kinetic analysis of supramolecular DNA–enzyme complexes

Prior to measuring the kinetics of surface-immobilized complexes **1**–**4**, we investigated, whether dissociation of DNA-immobilized conjugates occurs during the time span of a typical kinetic experiment. To this end, DNA-immobilized HRP-F5 was used as reporter. It was incubated in reaction buffer, and aliquots of the supernatant were analyzed for the presence of free conjugate, using an Amplex Red assay and external calibration curves for quantification of free HRP-F5 in solution. The measurements indicated that less than 3% of immobilized HRP had been dissociated from the carrier strands after 30 min (data not shown). We therefore estimated the influence of dissociation as negligible under the conditions used for kinetic analyses.

We then monitored the initial rates for the formation of resorufin as a consequence of the two-step reaction depicted in Fig. 1A.

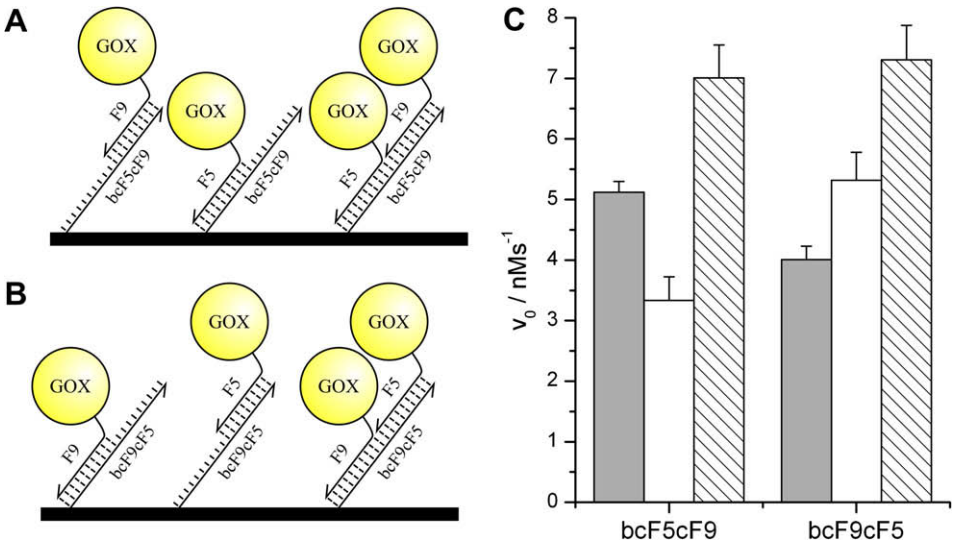

Fig. 3. Comparison of site-dependent hybridization efficiency. Two (30 fmol) microplate-immobilized capture sequences, bcF5cF9 (A) or bcF9cF5 (B), were allowed to bind GOX-F9 (grey bars), GOX-F5 (white bars), or a mixture of both conjugates (hatched bars). The hybridization efficiency was measured by assaying GOX activity, using 10 μM glucose, 20 μM Amplex Red in the presence of 1 nM native HRP (C). Note that the hybridization to the sequence stretch of the carrier closer to the surface is lower than to the stretch more distant from the surface. Note also that the presence of both conjugates only leads to approximately 80% of conjugate binding, as one would expect by addition of signals obtained from the single conjugate experiments (100%).

Various experiments were conducted using different amounts of capture oligomers immobilized in the microplate and fixed amounts of enzyme conjugates (150 fmol each). Initial rates were determined from the fluorescent signals of the resorufin product, and background corrected fluorescence values were converted into formation rates (υ_o in [nM/s]), using calibration curves of known concentrations of resorufin. The formation rates were then normalized by division by the concentration of capture oligomers to yield υ_o/c(carrier) values in [s^{-1}], which were plotted against the amount of immobilized carrier (see Supplementary material Fig. S2). Thus, the values represent the average transformation rates of the individual complexes, and higher values indicate more efficiently performing complexes.

The data determined for complexes **1**, **2**, and **3**/**4** indicated that heterodimeric complexes **1** and **2** revealed increased activity, predominantly in the case of low amounts of carrier strands (<150 fmol). In contrast, the reactivity of **1** and **2** was similar to that of control reaction containing **3**/**4**, when larger amounts of carrier were immobilized. To illustrate these effects more clearly, we normalized the reactivities of GOX–HRP complexes **1** and **2** against the control containing **3**/**4**, which was set as 100% (Fig. 4A). One can observe that the reactivity of the heterodimeric complexes **1** and **2** increased up to 180% as compared to **3**/**4**, while it leveled off at carrier amounts of about 100–150 fmol or higher. This result was expected because 150 fmol of the two DNA–enzyme conjugates were allowed to bind. Therefore, larger amounts of carrier will lead to the preferred formation of complexes, bearing only one of the two enzymes and, thus, to a decreased amount of heterodimeric complexes capable of substrate channeling. Vice-versa, lower amounts of carrier lead to preferred formation of doubly occupied carriers. Also, low carrier amounts statistically increase the distances in between complexes **3** and **4** in the controls, and thus, induce longer diffusion times which decrease overall bienzymatic conversion. In other words, the increase in relative signal observed for decreasing amounts of immobilized enzymes further supported our hypothesis that the immediate spatial proximity of GOX and HRP in complexes **1** and **2** enhances the coupled enzymatic activity.

Analogous experiments, carried out with conjugates GOX-T6-F9 and HRP-T6-F5, revealed similar effects (Fig. 4C). Here, the increase in reactivity of **1** and **2** in comparison to **3**/**4**, was even more pronounced (>300%). We attribute this observation to the increased hybridization efficiency and thus greater amount of heterodimeric complexes, formed due to the presence of the T_6-spacer (see above). It is also evident from Fig. 4A, and C that complex **1** revealed stronger activity than **2**. This result might be a consequence of the size of the two enzymes. GOX is a dimeric protein with a molecular weight of 160 kDa, while HRP is significantly smaller (approx. 40 kDa). Thus, the larger GOX is likely to hybridize more efficiently with the sterically better accessible sequence stretches distant from the surface (Fig. 3).

To further investigate the hypothetical channeling of H_2O_2 in the supramolecular complexes, a similar set of experiments was carried out in the presence of Catalase. Catalase efficiently converts H_2O_2 to water and molecular oxygen, revealing one of the highest turnover rates of all enzymes. We thus expected that Catalase should affect the controls in which H_2O_2 needs to diffuse in between **3** and **4** to a significantly larger amount than in the heterodimeric complexes **1** and **2**. In the latter, H_2O_2 should diffuse much faster between GOX and HRP due to the direct proximity with distances of less than 10 nm and thus, it should not be accessible to Catalase. As shown in Fig. S2 and Fig. 4B and D, we indeed observed stronger effects of Catalase on the controls (**3**/**4**) than on reactions containing **1** or **2**. However, activities were also dramatically decreased in the case of complexes **1** and **2**. This result suggests that diffusional transport of H_2O_2 also occurs in between individual complexes of **1** and **2** and it apparently contributes significantly to the global activity in a reaction vessel. The unexpectedly low effect of Catalase might also be associated with a side reaction, because this enzyme can convert Amplex Red to resorufin in the presence of molecular oxygen [26].

Conclusions

We here reported for the first time on the generation of heterodimeric enzyme complexes of GOX and HRP by means of DNA-directed assembly of enzyme–oligonucleotide conjugates. Investigation of the assembly process indicated that quantitative formation of ternary GOX–HRP–DNA complexes is hampered by the steric demand of the voluminous enzymes. Nonetheless,

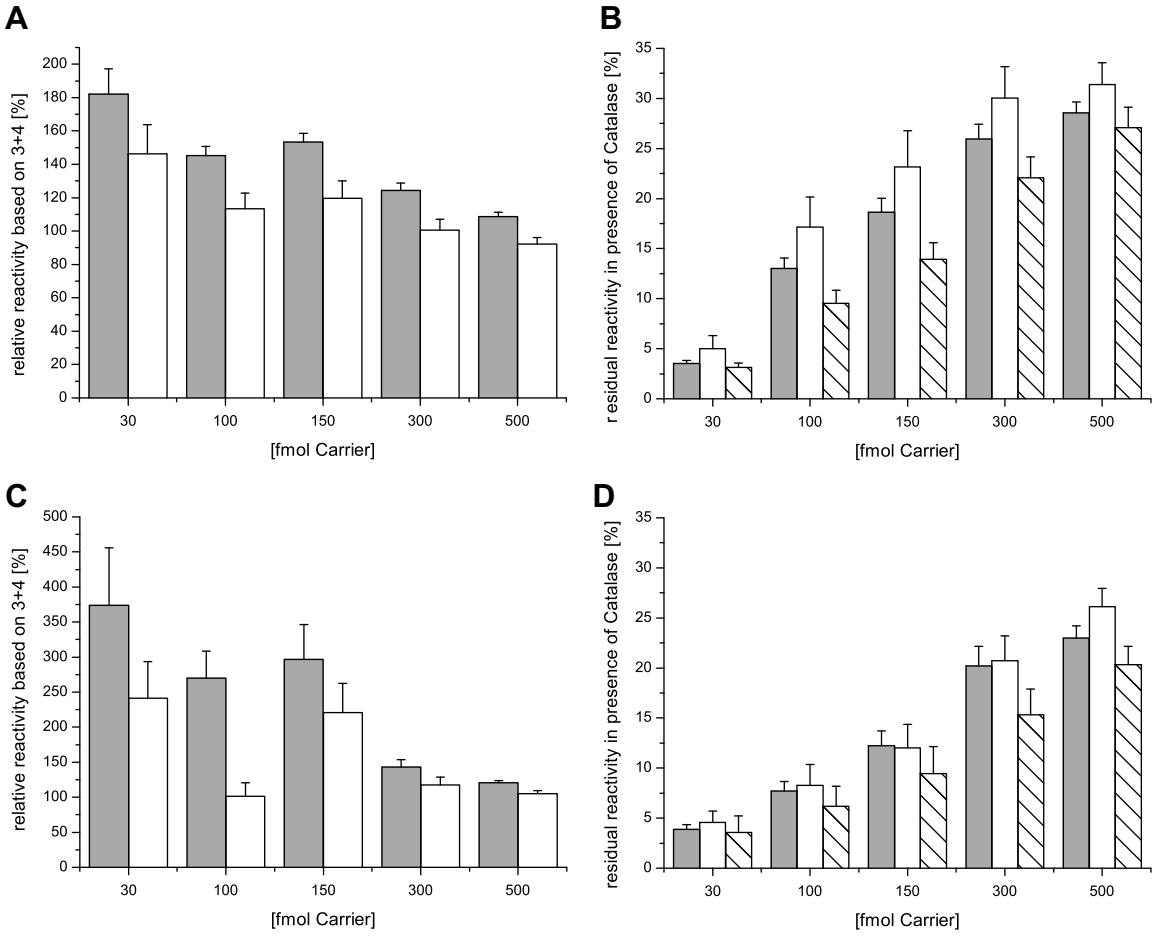

Fig. 4. Relative reactivities of GOX–HRP complexes **1** (grey bars) and **2** (white bars), normalized to the control complexes **3/4**. The charts show results obtained from independent experiments, using conjugates which either lack (A and B) or contain the T6-spacer (C and D). In charts B and D, the reactivity observed in the presence of Catalase was normalized to that of samples lacking Catalase, set as 100%. The hatched bars in B and D indicate the remaining activity of the control complexes **3/4**.

assembly of the complexes on microplate surfaces allowed us to assess kinetic rates, which indicated significant increase in the overall bienzymatic activity of those complexes, in which GOX and HRP were assembled in immediate proximity on the same DNA carrier strand. Although this data provided experimental evidence of channeling processes occurring in these complexes, the high quenching of the reaction by catalase suggested that inter-complex diffusion still plays a crucial role for overall activity also in these heterodimeric complexes. Therefore, further studies will concern, on the one hand, the development of DNA systems, which allow for more efficient assembly processes. On the other hand, elaboration of kinetic parameters, such as turnover rates (k_{cat}), and simulation of intermediate concentrations might be essential to understand the mechanistic processeses occurring in the supramolecular complexes [8]. We anticipate that further studies are not only useful to explore proximity effects in biochemical transformations, but the investigation of artificial multienzymes will also allow the development of novel catalysts for enzyme process technology, capable of regenerating cofactors, or to perform multistep chemical transformations of cheap precursors into drugs and fine chemicals.

Acknowledgments

This work was supported through founding of the Zentrum für Angewandte Chemische Genomik (ZACG), a joint research initiative founded by the European Union and the Ministry of Innovation and Research of the state Northrhine Westfalia. We thank Dr. Ljiljana Fruk and Max Glettenberg for help on the conjugate synthesis.

Appendix A. Supplementary data

Supplementary data associated with this article can be found, in the online version, at doi:10.1016/j.bbrc.2008.09.078.

References

[1] J.M. Berg, J.L. Tymoczko, L. Stryer, Biochemistry, fifth ed., W.H. Freeman, New York, 2002.
[2] C.O. Rock, S. Jackowski, Forty years of bacterial fatty acid synthesis, Biochem. Biophys. Res. Commun. 292 (5) (2002) 1155–1166.
[3] M. Ishikawa, D. Tsuchiya, T. Oyama, Y. Tsunaka, K. Morikawa, Structural basis for channelling mechanism of a fatty acid β-oxidation multienzyme complex, EMBO J. 23 (14) (2004) 2745–2754.
[4] M.F. Dunn, D. Niks, H. Ngo, T.R. Barends, I. Schlichting, Tryptophan synthase: the workings of a channeling nanomachine, Trends Biochem. Sci. 33 (6) (2008) 254–264.
[5] E.W. Miles, Tryptophan synthase: a multienzyme complex with an intramolecular tunnel, Chem. Rec. 1 (2) (2001) 140–151.
[6] M.A. Fischbach, C.T. Walsh, Assembly-line enzymology for polyketide and nonribosomal peptide antibiotics: logic, machinery, and mechanisms, Chem. Rev. 106 (8) (2006) 3468–3496.
[7] K.J. Weissman, R. Muller, Protein–protein interactions in multienzyme megasynthetases, Chembiochem 9 (6) (2008) 826–848.
[8] H.O. Spivey, J. Ovadi, Substrate channeling, Methods 19 (2) (1999) 306–321.
[9] L. Bulow, K. Mosbach, Multienzyme systems obtained by gene fusion, Trends Biotechnol. 9 (7) (1991) 226–231.
[10] I. Levy, O. Shoseyov, Cross bridging proteins in nature and their utilization in bio- and nano-technology, Curr. Protein Pept. Sci. 5 (1) (2004) 33–49.

[11] J.D. Kittendorf, D.H. Sherman, Developing tools for engineering hybrid polyketide synthetic pathways, Curr. Opin. Biotechnol. 17 (6) (2006) 597–605.
[12] C.M. Niemeyer, T. Sano, C.L. Smith, C.R. Cantor, Oligonucleotide-directed self-assembly of proteins: semisynthetic DNA-streptavidin hybrid molecules as connectors for the generation of macroscopic arrays and the construction of supramolecular bioconjugates, Nucleic Acids Res. 22 (25) (1994) 5530–5539.
[13] C.M. Niemeyer, Functional devices from DNA and proteins, Nanotoday 2 (2) (2007) 42–52.
[14] C.M. Niemeyer, J. Koehler, C. Wuerdemann, DNA-directed assembly of Bienzymic complexes from in-vivo biotinylated NAD(P)H:FMN oxidoreductase and luciferase, ChemBioChem. 3 (2002) 242–245.
[15] Z. Dai, J. Bao, X. Yang, H. Ju, A bienzyme channeling glucose sensor with a wide concentration range based on co-entrapment of enzymes in SBA-15 mesopores, Biosens. Bioelectron. 23 (7) (2008) 1070–1076.
[16] O. Kreft, M. Prevot, H. Mohwald, G.B. Sukhorukov, Shell-in-shell microcapsules: a novel tool for integrated, spatially confined enzymatic reactions, Angew. Chem. Int. Ed. Engl. 46 (29) (2007) 5605–5608.
[17] T.C. Logan, D.S. Clark, T.B. Stachowiak, F. Svec, J.M. Frechet, Photopatterning enzymes on polymer monoliths in microfluidic devices for steady-state kinetic analysis and spatially separated multi-enzyme reactions, Anal. Chem. 79 (17) (2007) 6592–6598.
[18] R. Baron, O. Lioubashevski, E. Katz, T. Niazov, I. Willner, Logic gates and elementary computing by enzymes, J. Phys. Chem. A 110 (27) (2006) 8548–8553.
[19] L. Fruk, J. Müller, C.M. Niemeyer, Kinetic analysis of semisynthetic peroxidase enzymes containing a covalent DNA–heme adduct as the cofactor, Chem. Eur. J. 12 (2006) 7448–7457.
[20] G.R. Schonbaum, S. Lo, Interaction of peroxidases with aromatic peracids and alkyl peroxides. Product analysis, J. Biol. Chem. 247 (10) (1972) 3353–3360.
[21] W. Franke, F. Lorenz, Zur Kenntnis der sog. Glucose-oxydase I, Liebig Annu. Chem. 532 (1) (1937) 1–28.
[22] C.M. Niemeyer, W. Bürger, R.M.J. Hoedemakers, Hybridization characteristics of biomolecular adaptors, covalent DNA–streptavidin conjugates, Bioconjugate Chem. 9 (2) (1998) 168–175.
[23] U. Feldkamp, R. Wacker, W. Banzhaf, C.M. Niemeyer, Microarray-based in vitro evaluation of DNA oligomer libraries designed in silico, ChemPhysChem. 5 (2004) 367–372.
[24] U. Feldkamp, H. Schroeder, C.M. Niemeyer, Design and evaluation of single-stranded DNA carrier molecules for DNA-directed assembly, J. Biomol. Struct. Dyn. 23 (6) (2006) 657–666.
[25] C.M. Niemeyer, L. Boldt, B. Ceyhan, D. Blohm, Evaluation of single-stranded nucleic acids as carriers in the DNA-directed assembly of macromolecules, J. Biomol. Struct. Dyn. 17 (3) (1999) 527–538.
[26] A.M. Vetrano, D.E. Heck, T.M. Mariano, V. Mishin, D.L. Laskin, J.D. Laskin, Characterization of the oxidase activity in mammalian catalase, J. Biol. Chem. 280 (42) (2005) 35372–35381.